STM JOURNALS

Journal of
Power Electronics & Power Systems

ISSN: 2249-863X (Online)
ISSN: 2321-4244 (Print)
Volume 14, Issue 3, 2024
September–December
DOI (Journal): 10.37591/JoPEPS

https://journals.stmjournals.com/jopeps

Review JoPEPS

Direct Determination of the Frequency-Dependent Transmission Constants of Non-Uniform Two-Port Networks

Mohamed Mostafa Saied*

Abstract

Due to space constraints and the expansion of electricity networks, transmission lines that cross close to one another are now commonplace. Power networks also commonly install higher operational voltage lines that share transmission corridors with lower voltage lines. Overhead transmission lines are the primary method for transmitting electrical energy across vast distances. This paper presents an efficient and direct technique for identifying the four frequency-dependent ABCD transmission constants of arbitrary non-uniform two-port networks. Special emphasis is devoted to non-uniform overhead transmission lines such as multi-span overhead lines and river crossings as well as the transitions from overhead lines and underground cables. The suggested approach is based on the numerical solution of the described system of simultaneous parametric differential and algebraic equations using the software Mathematica. The results include Laplace-domain expressions for the voltage and current distributions, from which the frequency-dependent line's input impedance and the ABCD constants could be easily determined. They are expressed in terms of the Laplace operators. The time-domain transient response of both the voltage and current distributions was obtained through the application of the efficient Hosono's algorithm for the numerical Laplace inversion. The computed results address the cases of short-circuit, open-circuit, pure resistive as well as resistive/inductive line loading conditions. The impedance plots could exhibit several series and parallel resonance frequencies and the corresponding impedance values. The relevant impedance locus plots are also presented and discussed. The suggested approach is applied to a typical multi-span overhead high-voltage transmission line comprising a large number (tens or even hundreds) of supporting towers.

Keywords: Electromagnetic, transients, simulation, high-voltage lines, differential equations, parametric ND solve, Mathematica, numerical solutions, two-port networks, frequency response, laplace transform

INTRODUCTION

Transmission lines that pass near one another have become a result of power networks growing larger and space limitations. In addition, power networks frequently add lines with higher operating voltages that share transmission corridors with lines with lower voltages. Overhead transmission lines are the main means of sending electrical energy across long distances. Transmission line disruptions, such as lightning or switching, can cause overvoltage transients, which can then spread to other parts of the power system [1–3].

Consequently, inadequate countermeasures may lead to device failure and breakdown of electrical insulation. Therefore, while building and analyzing power systems, precise electromagnetic transient (EMT) modeling of the transmission lines is crucial.

***Author for Correspondence**
Mohamed Mostafa Saied
E-mail: mmsaied002@gmail.com

Professor (Emeritus), Department of Electrical Engineering, Kuwait University, Independent Researcher, IEEE Life Senior Member, Giza, Cairo, Egypt

Received Date: October 16, 2024
Accepted Date: October 20, 2024
Published Date: October 25, 2024

Citation: Mohamed Mostafa Saied. Direct Determination of the Frequency-Dependent Transmission Constants of Non-Uniform Two-Port Networks. Journal of Power Electronics & Power Systems. 2024; 14(3): 1–8p.

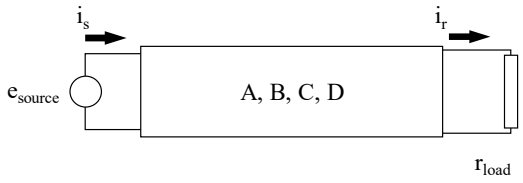

Figure 1. A two-port network.

A transverse electromagnetic (TEM) mode of propagation is assumed by the multiconductor transmission line (MTL) theory, which forms the basis of conventional transmission line components in electromagnetic transient (EMT) simulators that are used to examine the transient behavior of power networks. These models typically use the Carson-Pollaczek formula to account for frequency-dependent ground losses [4]. However, these requirements only apply to uniform transmission lines that are infinitely long and normally not met in actual implementations. To simulate the propagation of non-TEM mode waves in transmission lines, EMT simulators have integrated models based on the Method of Moments with Surface Impedance Operator (MoM-SO). However, MOM-SO cannot be used for non-uniform or finite-length conductors because it is based on circuit theory. In addition, non-uniform soil characteristics, line sag, and proximity effects cannot be modeled using traditional terminal-based uniform transmission line models employed in EMT simulators. Therefore, to effectively mimic the transient behavior of current transmission networks, EMT simulators must consider the effects of nonuniformities of finite-length transmission lines. FDTD algorithms determine the voltage and current of each space segment at each time-step field-to-line coupling after discretizing the structure into a finite number of space segments and can easily model transmission lines with non-uniform external field excitation and non-uniform line characteristics. The fact that FDTD models require more calculations at each time step than traditional terminal-based models used for uniform lines is a drawback [14]. The advancement of communication systems in recent years has led to major problems with high-speed printed circuit boards, including increased integration levels and signal transmission speeds, as well as electromagnetic interference between circuits. It is often known that electromagnetic crosstalk between passive devices is a significant problem for signal integrity in high-speed circuits.

Any linear two-port network can be described by the two equations.

$$Vs=A.Vr+B.Ir \quad (1)$$

$$Is=C.Vr+D.Ir \quad (2)$$

Where, *Vs* and Is voltage and current at the sending end of the network, respectively, and *Vr* and Ir are the corresponding quantities at the receiving end.

A, B, C, and *D* are the transmission constants of [four]. It can be seen that.

$A=(Vs/Vr)$ and $C=(Is/Vr)$ with open receiving-end terminals. (3)

$B=(Vs/Ir)$ and $D=(Is/Ir)$ (4)

with short-circuited receiving end as shown in Figure 1.

The network's input impedance is, therefore,

$$Zinput=(Vs/Is)=(A.Zload+B)/(C.Zload+D) \quad (5)$$

Where, *Zload* is the network's termination impedance

METHOD OF ANALYSIS

The analysis starts by writing the network's system of equations, in which the differentiation with respect to time is replaced by multiplication by (jω) in the frequency domain. The next step was to apply the *Mathematica* statement (ParametricNDSolve). The term {w} is used as a parameter [5–9].


```
sol = ParametricNDSolve[{D[v[x ], x] == - ind[x ] * (I*w) * i[x], D[i[x ], x] == - cap[x ] * (I*w) * v[x],
    v[0] == esource[I*w], v[length ] == rload*i[length] }, {v , i }, {x, 0, length}, {w},
  AccuracyGoal → 1, MaxSteps → Infinity]
voltage[x_, s_] := v[s / I][x] /. sol
current[x_, s_] := i[s / I][x] /. sol
```

Figure 2. A segment of the *Mathematica* Code.

```
amn[1] = 63; amn[2] = 57; amn[3] = 42; amn[4] = 22; amn[5] = 7;
amn[6] = 1; ll = 29; Do[amn[kk] = amn[kk] / (2^6), {kk, 1, 6}] // N;
tmax = 0.0015 ; tmin = 0; nn = 150 ; dt = (tmax - tmin) / nn ;
t[k_] := k*dt + tmin // N;
s[mm_, ii_] := (5 / t[mm] + I*(ii - 0.5)*Pi / t[mm]) // N;
x = length / 2 // N
Table [
 ((Sum [N[(-1)^ii * Im[voltage [x, s[mm, ii]]]], {ii, 1, 29}] +
     Sum [N[(-1)^(ll + 29) * amn[ll] * Im[voltage [x, s[mm, (ll + 29)]]]], {ll, 1, 6}]) * (E^5) / t[mm]),
 {mm, 10, nn}]
ListPlot [%, PlotRange -> All, Joined -> True, GridLines → Automatic , Frame → True ,
 FrameLabel → {"Time , 1 div .=10 micros .", "voltage at x=length /2, v"}, PlotStyle → {Thickness [0.008 ]}]
x = length / 2 // N
```

Figure 3. The Hosono algorithm.

The segment below shows the solution of a non-uniform transmission line transient with location-dependent inductance *ind[x]* and capacitance *cap[x]*. References [10, 11] give a detailed derivation of these distributed circuit parameters. The terms *length* and *rload* are the line's total length and the termination resistance, respectively. The line termination resistance *road* can be substituted with either zero or infinity to determine the *ABCD* transmission constants according to the above-mentioned definitions [12].

The output results are the voltage and current as functions of location *x* measured from the source. Thus, they can be numerically presented in Figures 2 and 3. Laplace-inverted to obtain them in the time-domain, [13]. The shortcode listed in Figure 3 the code of the famous Hosono algorithm. It should be noted that owing to the assumed linearity of the network, the time waveform of the source voltage will not affect the results of the input impedance or the network's transmission constants.

SAMPLE RESULTS

The presented technique is applied to an example dealing with a 15-km non-uniform overhead transmission line comprising 50 tower spans, 300 m each. The voltage source initiating the transient was assumed to be a ramp function.

$$esource(t) = (10^8\, t) \text{ Volts}, \tag{6}$$

Where, *t* is the time in seconds.

The linearly increasing source voltage reaches the value 140-kV after the considered time range of 1400 μsec.

Case Study A: The Non-uniform Line Terminated by a 100-Ohm Resistance

The transient responses of the voltage and current at the line's middle point (*x*=7.5 km) are illustrated in Figures 4(a) and (b), respectively. Both exhibited an almost linear increase over time. The plots also include several high-frequency components. This can be attributed to numerous wave reflections at the load, source, and tower locations. The values at t=1400 μsecare approximately 140 kV and 1500 A, respectively.

The frequency dependence of the impedance input of the line is shown in Figure 5. They depict, respectively, its magnitude, phase angle, and locus plot over the frequency range from zero to 30 kHz. The magnitude fluctuated between 100 Ω and 1150 Ω. at different series and parallel resonance frequencies. The impedance angle changes with the frequency between +55 and -55 degrees. This can be seen by inspecting the locus plot (Figure 5(c)).

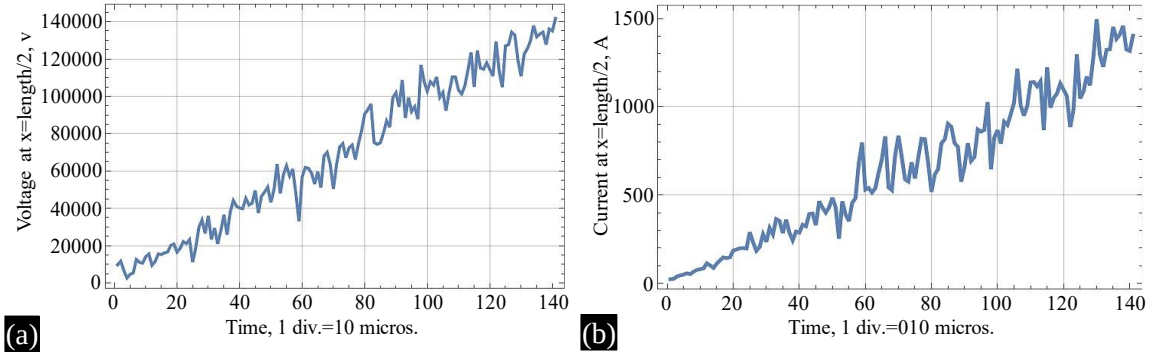

Figure 4. The voltage and current transients at the line's middle point. The line is terminated by a 100-Ohm resistance. (a) The voltage at the line's middle point, (b) The current at the line's middle point.

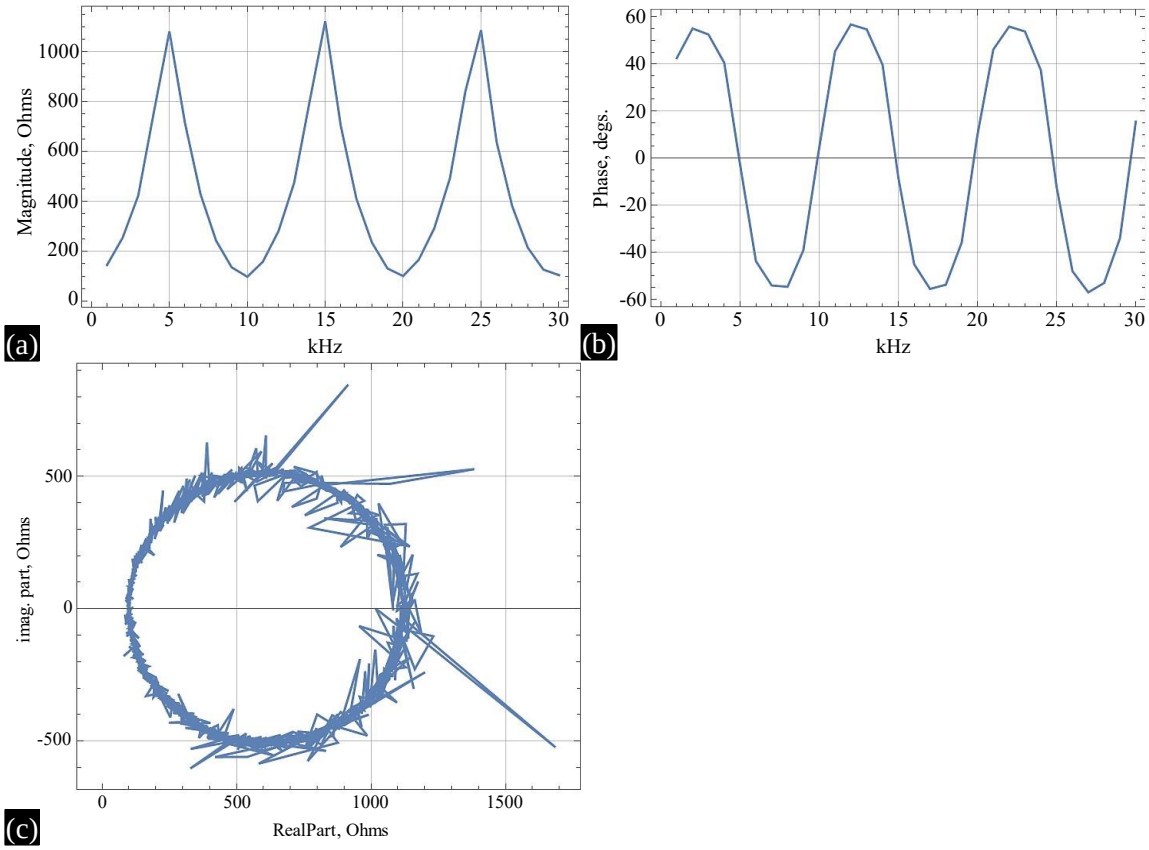

Figure 5. The computed results of Case Study A. (a) magnitude of the input impedance, (b) phase angle of the input impedance, (c) the input impedance's locus plot. The line is terminated by a 100-Ohm resistance.

Case Study B: The Non-uniform Line is Short-Circuited

The computed results of the line's receiving-end current during the time range ending at t= 3 ms, the input impedance magnitude, and the frequency locus plot are depicted in plots (a), (b), and (c) of Figure 6, respectively. The load current starts with an initial value of zero and increases rapidly to values above 20 kA at a time point *t* close to 3 ms. This agrees with the numerical inversion of the well-known expression *esource(s)/B(s):*

The impedance magnitude exhibits several peaks above 10 K Ohms at parallel resonance frequencies. These extreme values are primarily due to the very large reactive components. This is evident from the locus plot (Figure 6(c)). There are also many series resonances characterized by very small impedance values.


```
In[•]:= tau = 5 * 10^-5;
        zo = 360;
        InverseLaplaceTransform[(10^8 / s^2) / (360 * Sinh[tau * s]), s, 0.003]
Out[•]= 24997.7
```

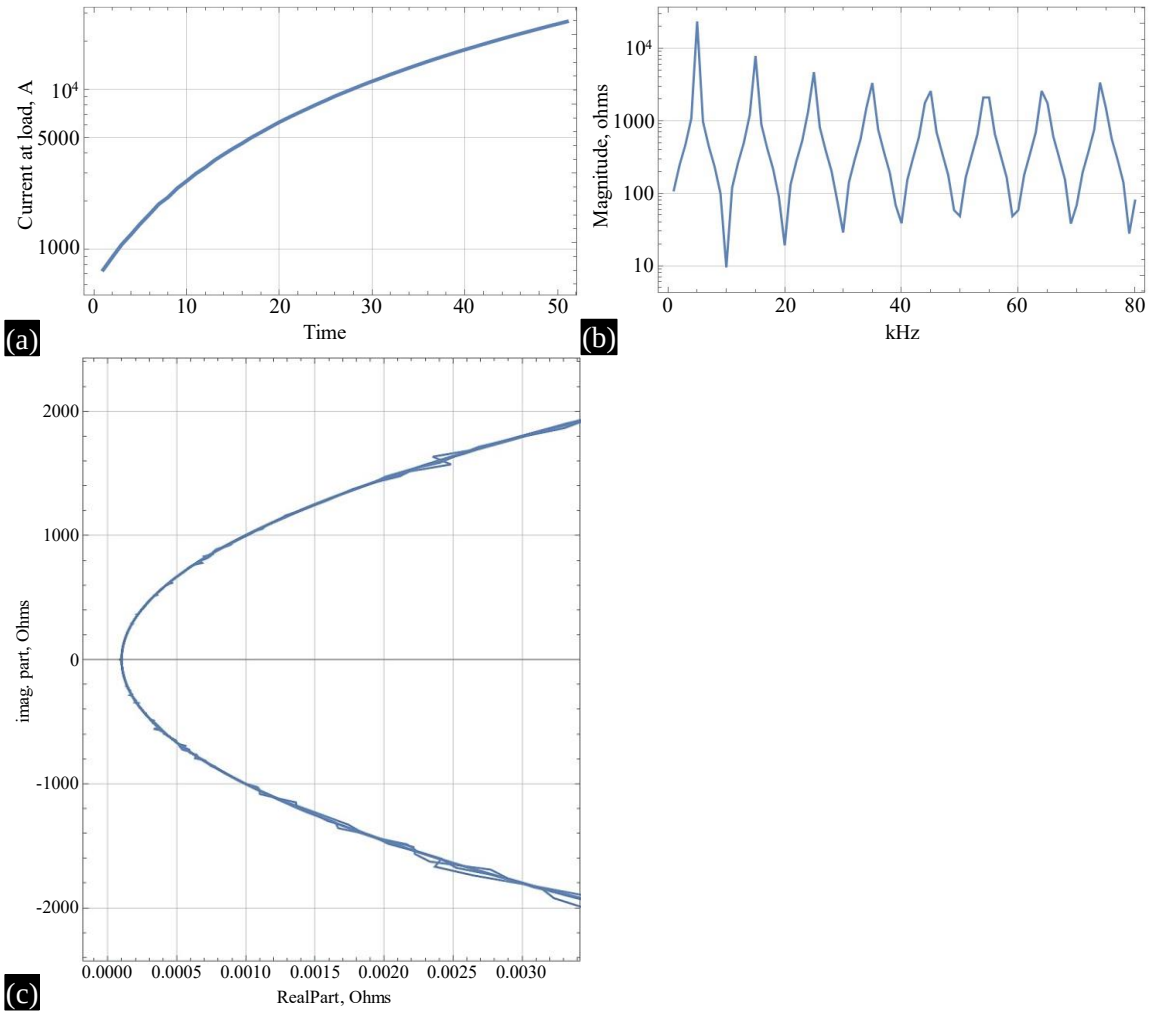

Figure 6. The load current, the input impedance's magnitude, phase angle, and its locus plot. The line is short-circuited. (a) The receiving-end (load) current over the time range ending at 3 ms, (b) The magnitude of The line's input impedance under short-circuits conditions, (c) the Locus plot of the input impedance.

Case Study C: The Non-uniform Line is Open-Circuited

The transient voltage developed at the receiving end of the unloaded non-uniform line is shown in the plot (Figure 7(a)). It increased from an initial value of zero to a value slightly less than 300-kV at 3 ms. This is in full agreement with the numerical inversion of the well-known expression *esource(s)/A(s):*

```
In[•]:= tau = 5 * 10^-5;
        zo = 360;
        InverseLaplaceTransform[(10^8 / s^2) / (Cosh[tau * s]), s, 0.003]
Out[•]= 299520.
```

The frequency dependence of the input impedance over the frequency range of 0–60 kHz is shown in the plot (Figure 7(b)). It assumes an infinity. A large DC value was expected. Moreover, it exhibits several series and parallel resonances. The first series and parallel resonances occur at 5 and 10 kHz, respectively. Their corresponding impedance values are 2 and 10000 Ω, respectively, which is also recognizable from the locus plot as shown in Figure 7(a)–(c).

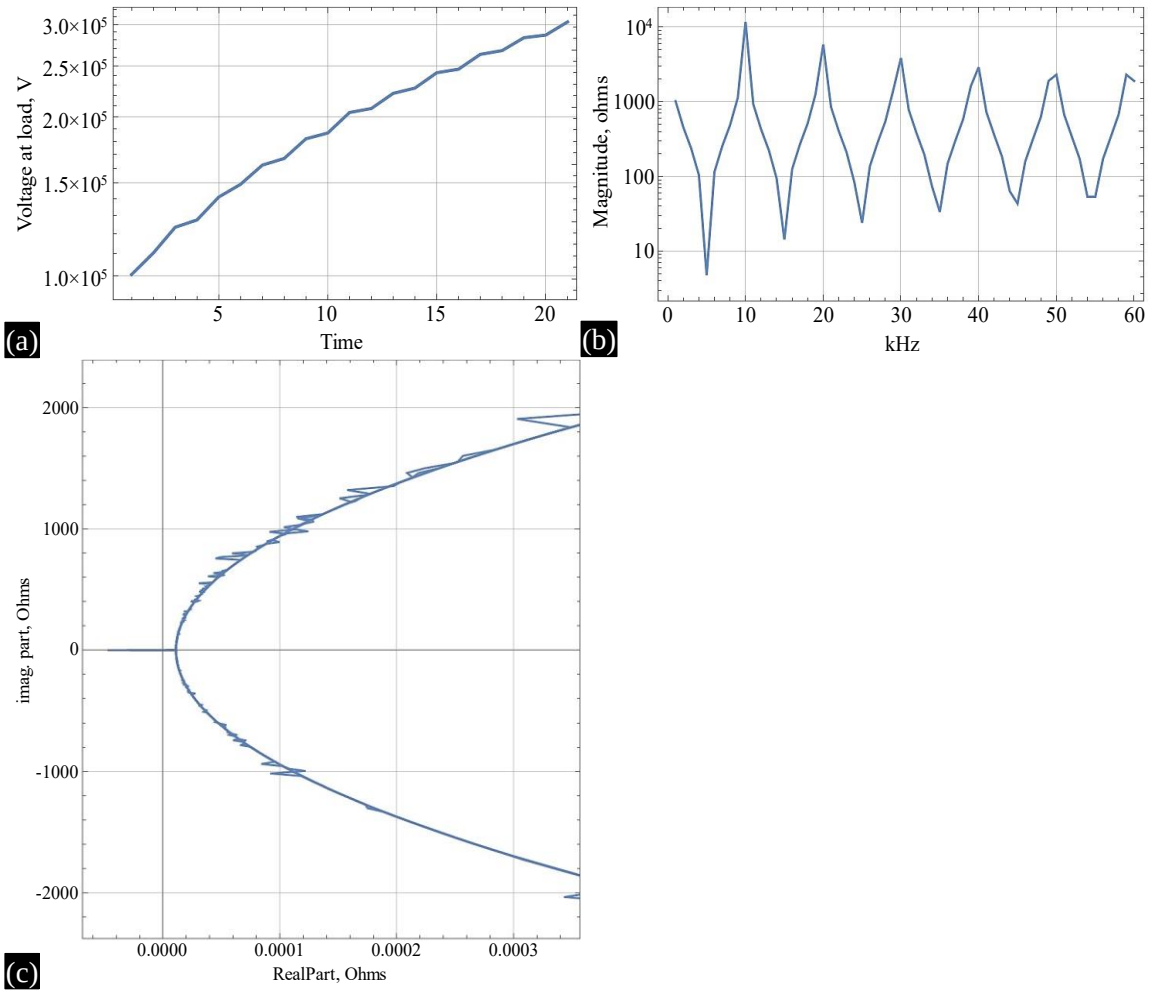

Figure 7. The load voltage, the input impedance's magnitude, phase angle, and its locus plot over the frequency range (0–60 kHz). (a) The voltage at the line's open-ended terminals, (b) The magnitude of The line's input impedance under open-circuit conditions over the frequency range (0–60 kHz), (c) The impedance locus plot.

Case Study D: The Non-uniform Line's Load is Resistive/Inductive

This section addresses the case in which the line is loaded by a 1000 Ohm resistance in series with a 21 mH inductance. The line is open-circuited. The results are shown in Figure 8. As expected, plots in Figure 8(a) and (b) indicate that the final values of the load voltage and current are 100 V (which is the assumed DC source voltage) and 0.1 A, respectively.

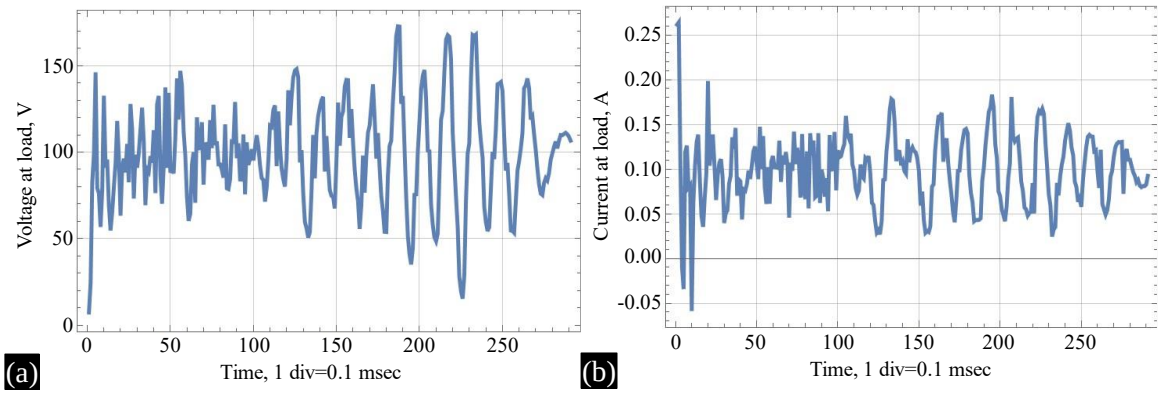

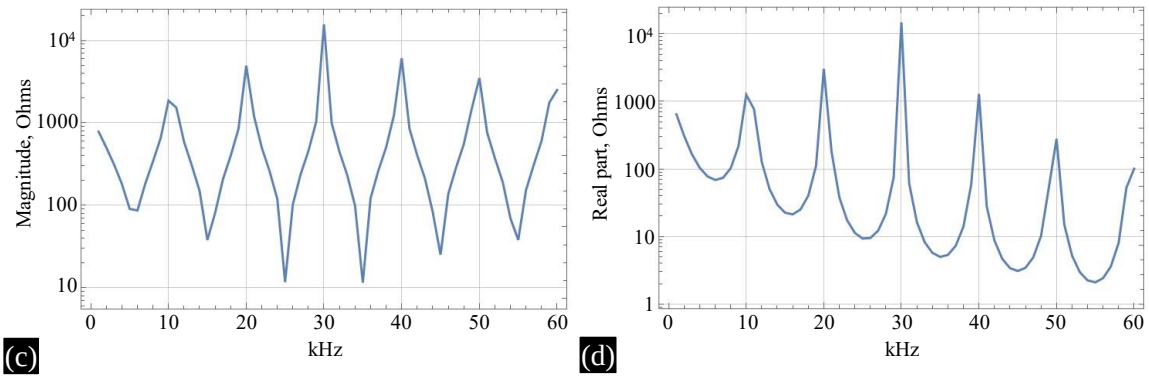

Figure 8. The load voltage, load current, the input impedance's magnitude, and its real part over the frequency range (0–60 kHz). (a) The load voltage, (b) The load current, (c) The magnitude of input impedance, (d) The real part of input impedance.

The line was loaded with a series connection with 1000 Ω resistance and 21 mH inductance. As the two plots in Figure 8(c) and (d) indicate, the input impedance at zero frequency is purely resistive and equal to the initially assumed resistance of 1000 Ω. The impedance exhibited several series and parallel resonances at the frequencies of 5, 10, and 15. kHz, etc.

CONCLUSIONS

The proposed technique proved to be helpful for the direct determination of the frequency-dependent transmission constants of non-uniform two-port networks. Special emphasis was placed on the analysis of overhead transmission lines comprising a large number of suspension towers. The effects of their lengths and loading conditions on the voltage and current transients are described. Moreover, the frequency dependence of the network input impedance and its *ABCD* transmission constants were investigated. The analysis and associated computer code can also yield different resonance frequencies for the considered networks. The computed results of several case studies demonstrated the validity, applicability, ease of implementation, and accuracy of this user-friendly procedure.

REFERENCES

1. Greenwood A. Electrical Transients in Power Systems. New York: John Wiley & Sons, Inc.; 1991. Chapter 11.
2. Begamudre RD. Extra high voltage transmission engineering. 2nd ed. Wiley Eastern Limited; 1990. p. 31–3.
3. Bewley LV. Travelling Waves on Transmission Systems. New York (NY): Wiley; 1963.
4. Grainger J, Stevenson W. Power System Analysis. McGraw-Hill; 1994. International edition. Chapter 6 & Appendix A.
5. Morched A, Gustavsen B, Tartibi M. A universal model for accurate calculation of electromagnetic transients on overhead lines and underground cables. IEEE Trans Power Deliv. 1999;14:1032–8.
6. Saied MM. Effect of cable sections on the electromagnetic transients in power networks. Electric Mach Power Syst. 1988;15:17–35. DOI: 10.1080/07313568808909311.
7. Meredith RJ. EMTP modeling of electromagnetic transients in multimode coaxial cables by finite sections. IEEE Power Eng Rev. 1997;17:69–70. DOI: 10.1109/MPER.1997.560719.
8. Saied M. Transient response of networks to nonstandard waveforms: Analysis and case studies. Int J Analog Integr Circ. 2022;8(1):25–32.
9. Saied M. Electromagnetic transients on power lines due to multi-pulse lightning surges. CIGRE Session 2002; No. 33–101. Paris.
10. Saied M. Effect of the conductor sag on the electromagnetic transients in high voltage lines. Int J Analog Integr Circ. 2024;10:8–16.
11. Saied M. Appendix: The combined effect of both the conductors' sag and the initiating stimuli on the electromagnetic transients in high voltage lines. Int J Analog Integr Circ. 2024;10:8–16.

12. Wolfram Mathematica. Tutorial collection: Advanced numerical differential equation solving. Wolfram Research; 2008. Available from www.wolfram.com/learningcenter/tutorialcollection/AdvancedNumericalDifferentialEquationSolvingInMathematica. Accessed November 2019.
13. Montella C, Diard J-P. (2015). Comparing four methods of numerical inversion of Laplace transforms (NILT) [Online]. Wolfram Demonstrations Project. Available from: https://demonstrations.wolfram.com/ComparingFourMethodsOfNumericalInversionOfLaplaceTransformsN/
14. Gunawardana MS. Scattering-theory-based methodology for electromagnetic transient analysis of nonuniform frequency-dependent transmission line structures [dissertation]. Winnipeg, Canada: University of Manitoba; 2022. Available from: https://mspace.lib.umanitoba.ca/items/cfec0191-c942-411e-9ff8-9d73704808fc

